# scientific reports

OPEN

# Gallic and glycyrrhetinic acids prevent azithromycin-induced liver damage in rats by mitigating oxidative stress and inflammation

Marwa Ahmed Mohamed Ali[1], Asmaa Ibrahim Matouk[2], Alaaeldin Ahmed Hamza[3✉], Amr Amin[4✉] & Gehan Hussein Heeba[2]

Natural products like gallic acid (GA), a phenolic compound, and glycyrrhetinic acid (GLA), a pentacyclic triterpene, have been shown to exhibit antioxidant, ant-inflammatory, and hepatoprotective properties. This study aims to investigate the protective effects of GA, GLA and their combination and to explore their underlying mechanisms against acute liver damage induced by azithromycin (AZM) in rats. Seven groups of male Wistar rats were used namely control, GA, GLA, AZM, AZM + GA, AZM + GLA, and AZM + GA + GLA groups. We treated the rats for 21 days, administering GA and GLA at 50 mg/kg one week prior to AZM (30 mg/kg). Serum levels of aspartate aminotransferase, alanine aminotransferase, and alkaline phosphatase in rats AZM-induced and pre-treated with of GA, GLA, and combination therapy were much lower than those in the AZM group Elevated levels of glutathione, catalase, and superoxide dismutase in preventive rats demonstrated that GA, GLA, and their combinations notably reduced AZM-induced malondialdehyde levels, an oxidative stress marker, improving the antioxidant system in those groups. Furthermore, GA, GLA, and their combinations reduced pro-inflammatory cytokines, such as tumor necrosis factor-α and nuclear factor kappa beta (NF-kB), thus reversing hepatic inflammation. We also discovered that AZM down-regulated nuclear factor erythroid 2-related factor 2 (Nrf2), and that its normal levels were restored post treatments with GA, GLA, and their combination suggesting a Nrf2 signaling pathway-mediated prevention of AZM-induced liver damage. In conclusion, GA, GLA, and their combination protected rats against AZM-induced liver injury through their demonstrated ability to lower oxidative stress and inflammation by preventing downregulation of Nrf2 and upregulation of NF-kB. After determining their efficacy and safety in clinical settings in future studies, GA and GLA could potentially make useful therapeutic drugs to mitigate AZM-induced hepatotoxicity.

**Keywords** Azithromycin, Gallic acid, Glycyrrhetinic acids, Liver damage, Nrf2, NF-kB

Drug-induced liver injury (DILI), while uncommon, can lead to potentially life-threatening consequences including elevated liver enzymes, acute liver failure, and even mortality[1]. Azithromycin (AZM), a macrolide antibiotic, is among the top ten medications causing DILI[2]. It effectively treats genitourinary infections, enteric diseases such as typhoid, and respiratory conditions like pneumonia[3,4], indicating its broad-spectrum antibacterial activity against both gram-positive and gram-negative bacteria. Moreover, AZM has demonstrated therapeutic potential in manging cure for a wide range of illnesses, including viral infections such as COVID-19 [4,5,6].

Scientific research has undoubtedly established two recognized adverse effects of AZM administration: hepatotoxicity and cardiotoxicity[7,8]. Li et al.[9] conducted an extensive study on hepatotoxicity in animals, and Ellison and Blackwell[10] observed it in humans. Clinical studies have confirmed that AZM can have serious negative effects on both adults and children, such as cholestasis, jaundice, and liver dysfunction[1,11]. Research has documented cases of acute cholestatic hepatitis developed within the first three weeks of starting AZM medication[1,11]. According to Martinez et al.[12], liver damage typically appears within one to three weeks after

[1]Abu Qurqas Health Administration, Minia Directorate of Health, Ministry of Health, El-Minia 61611, Egypt. [2]Department of Pharmacology and Toxicology, Faculty of Pharmacy, Minia University, El-Minia, Egypt. [3]Biology Department, National Organization for Drug Control and Research, Giza 12611, Egypt. [4]College of Medicine, University of Sharjah, Sharjah 27272, UAE. ✉email: alaa17mm@gmail.com; a.amin@sharjah.ac.ae

starting medication. While AZM often causes mild liver damage, there are cases when it can result in significant liver damage, requiring a liver transplant and potentially leading to abrupt liver failure[13,14]. Recognizing these potential risks and maintaining a diligent attitude towards detecting any indications of liver damage in patients receiving AZM treatment, is of utmost importance. We do not fully understand how AZM affects hepatic tissue, but we hypothesize that oxidative stress and inflammation play a significant role.

Currently, there are limited therapeutic and preventive options for liver disease, despite its global prevalence and significant contribution to mortality rate worldwide. People widely recognize oxidative stress and inflammation as major factors in liver disease development[15]. Researchers and healthcare professionals are increasingly focusing on naturally occurring polyphenol compounds to reduce the harmful effects of various drugs and environmental pollutants[16]. Recently, these compounds have gained significant attention thanks to their diverse pharmacological properties and therapeutic potential[17]. Gallic acid (GA), a naturally occurring phenolic compound with potent antioxidant properties, is characterized by its relatively low molecular weight and is chemically known as 3,4,5-trihydroxybenzoic acid[18]. GA has several biochemical and pharmacological characteristics, such as anti-inflammatory, antibacterial, antioxidant, cardioprotective, antiviral, and anticancer effects[19,20]. This natural phenolic compound is found in a variety of plant-based sources including apple peels, walnuts, mangoes, grapes, and green tea. GA exhibits significant hepatoprotective properties[19,20], demonstrating its efficacy in combating different liver-damaging agents including carbon tetrachloride (CCL4)[21], nitroso diethylamine[22], lead[23], tert-butyl hydroperoxide[24], bisphenol[25], ethanol[26], thioacetamide[27], and cadmium[28]. GA's biological activities, particularly its antioxidant properties, protect human cells and tissues from oxidative stress-induced damage[18,20]. Glycyrrhiza species, commonly known as licorice, is the primary source of pentacyclic triterpene glycoside[29]. The root of licorice is the main source of glycyrrhetinic acid (GLA), a bioactive pentacyclic triterpene[29,30]. Licorice yields two isomers of glycyrrhetinic acid: 18β1-glycyrrhetinic acid and 18α-glycyrrhetinic acid[30]. These compounds exhibit a range of pharmacological characteristics including antiviral, anti-inflammatory, antifibrotic, and antioxidant activities[29]. Recent studies have shown that GLA can protect liver cells from damage induced by various toxins such as CCL4 [31,32], 2-acetylaminofluorene[33], cyclophosphamide[34], methotrexate[35], and alpha-naphthyl isothiocyanate[32]. The findings indicate that GLA possesses hepatoprotective characteristics and can mitigate liver damage induced by various harmful chemicals.

Iranshahy et al.[36] showed that nuclear factor Erythroid 2-Related Factor 2 (Nrf2) plays a critical role in protecting the liver from drug-induced toxicity. Their study revealed that Nrf2 regulates the expression of genes dependent on antioxidant response elements (ARE), which are essential for maintaining cellular resilience against oxidative stress. The activation of Nrf2 triggers the transcription of antioxidant and cytoprotective enzymes, including SOD, catalase, heme oxygenase 1, NAD(P) H, quinone oxidoreductase 1, and NAD(P)[36], thereby enhancing the cell's defense mechanisms.

Many natural products have demonstrated hepatoprotective properties[20,29,30]. In this study, we focused on two main classes of bioactive compounds: Phenolic acids, such as GA, and triterpenoid compounds, such as GLA[20,29,30]. Notably, Nrf2 activation appears to be a key mechanism underlying the hepatoprotective effects of these natural compounds[30,36]. Licorice-derived compounds like GLA, when used in combination with other therapeutic agents, have been shown to enhance liver protection against DILI[29]. Accordingly, this study aims to evaluate the protective effects of AZM, GA, GLA, and their combinations in mitigating acute hepatotoxicity in male Wistar rats. The present findings suggested that GA, GLA, and their co-administration protect the liver by modulating oxidative stress and inflammatory pathways.

## Materials and methods
### Chemicals
Thiobarbituric acid, pyrogallol, and 18β1-glycyrrhetinic acid (CAT# G10105) and gallic acid (CAT# G7384) were obtained from Sigma-Aldrich (St. Louis, MO, USA). The AZM (Xithrone, 500 mg, 211515) was acquired from Amoun, located in El Obour City, Qalyubia, Egypt. The inquiry selected the highest analytical grade for all other substances.

### Animals
The study included a sample of 42 male albino Wistar rats, with weights ranging from 180 to 220 g. These rats were obtained from the experimental animal house at Nahda University, Beni Suef. The rats were put into 7 experimental groups using random assignment. To calculate the effect size, we utilized previously published data from Paulose et al.[37], with a power of 0.9 and a significance threshold of 0.05. Before commencing the experimental procedures, the rats were provided with one week to adapt to the laboratory setting. The subjects were kept in plastic enclosures with regulated humidity ($55 \pm 1\%$), temperature (%), and a light-dark cycle of 12 h each. The rats were given a standard commercial diet and had unrestricted access to water.

### Ethics declaration
Animal experiments were conducted in compliance with international standards for the care and utilization of laboratory animals (National Research Council (US) Committee for the Update of the Guide for the Care and Use of Laboratory Animals, 8th edition. Washington (DC): National Academies Press (US); 2011). All experimental protocols were approved by the Research Ethics Committee for the care and use of laboratory animals at Minia University, Faculty of Pharmacy (ethical approval number: 2301004). In addition, all experimental protocols were reported following the relevant guidelines and regulations reported in ARRIVE guidelines 2.0. (https://arriveguidelines.org).

## An experiment's design

The experiment involved randomly assigning rats to different groups. The study involved seven groups, each containing six rats. The control group of rats received a solution of water and tween 80 drops (5 mL/kg/day) for 21 days. The rats in the GA group received a daily dosage of GA orally (50 mg/kg/day, dissolved in 5 mL/kg water containing Tween 80 droplets) for 21 days. Rats in the GLA group received GLA orally (50 mg/kg/day) in a solution of water and Tween 80 drops for 21 days. The AZM group was administered a solution of water mixed with Tween 80 drops orally (5 mL/kg/day) for 21 days. Starting on the eighth day, these rats were also given AZM orally at a dose of 30 mg/kg/day in a solution of water and Tween 80 drops for 14 days. The rats in the GA + AZM group were administered oral GA (50 mg/kg/day) for 21 days. On the eighth day, the rats received oral AZM (30 mg/kg/day, in a solution of water and Tween 80 drops) for a duration of 14 days. The group of rats known as GLA + AZM were administered GLA orally at a dosage of 50 mg/kg body weight for 21 days. On the eighth day, they received oral administration of AZM at a dosage of 30 mg/kg/day in a solution of water and Tween 80 drops for 14 days. The group of rats labeled as GA + GLA + AZM were administered both GA and GLA orally for 21 days, with a dosage of 50 mg/kg body weight for each substance. Starting on the eighth day, we administered AZM orally at a daily dose of 30 mg/kg for 14 days.

The doses of GLA and GA were chosen according to prior research that has shown their hepatoprotective effects against different substances[35,38]. In addition, a liver injury model generated by AZM was established according to pilot experimental trials as well a as to previously described by Paulose et al.[37].

## Sample collections and preparations

The rats were anaesthetized using a ketamine/xylazine (60/5 mg/kg, i.p.) 24 h after the final treatment. Blood samples were then taken from the retro-orbital plexus. The rats were euthanized through cervical dislocation following blood extraction. Subsequently, the liver was promptly extracted, rinsed with cold normal saline, and weighed. To conduct histological studies, a section of liver tissue was promptly immersed in a 10% buffered formalin solution. The liver tissues were homogenized using a Tris-HCL buffer at a ratio of 1:5 (liver tissue to buffer) with a concentration of 150 mM and a pH of 7.4. The homogenate was partitioned into vials and stored at a temperature of -80 °C. Using appropriate buffers, dilutions were prepared from the latter to test the amounts of GSH, LP product MDA, total proteins, and SOD and CAT activity. Centrifuge tubes were used to collect blood, which was then subjected to centrifugation for 20 min at a speed of 3000 revolutions per minute in a refrigerated centrifuge set at a temperature of 4 °C. This process was carried out to extract serum. Serum samples were utilized for the measurement of the levels of ALT, AST, ALP and albumin.

## Biochemical and histopathological assays

### Assessment of liver toxicity biomarkers

Assessment of liver injury biomarkers was conducted by measuring the levels of alanine aminotransferase (ALT), aspartate aminotransferase (AST), alkaline phosphatase (ALP), and albumin. Commercial kits from BIOMED in Al Asher Men Ramadan, Cairo, Egypt, were used, following the manufacturer's instructions.

### Histopathological analysis using haematoxylin and eosin staining

According to the procedure outlined in Bancroft's[39] methodology, the preserved samples were clipped, cleaned, dried using progressively stronger alcohol solutions, treated with xylene to remove impurities, encased in paraffin, and then cut into sections measuring 4–6 micrometres in thickness. The sections were subsequently stained using the hematoxylin and eosin (H&E) method. Histological evaluations were conducted by analyzing five distinct regions of each liver sample at a random 200x magnification. The evaluations were centred around the identification of histological alterations, including hydropic degeneration, localized necrosis, vascular congestion, and inflammatory cell infiltrations. The magnitude of these alterations was assessed using a grading method employed in a prior investigation conducted by Ibrahim Fouad and Ahmed[40]. The grading system had a range of values from 0 to 3, and each value had a specific connotation. The grades were determined as a percentage to measure the extent of the detected histopathological alterations. Grades 0 (zero) signified a negative outcome, whereas Grades 1 (0–30%), 2 (31–50%), and 3 (51–100%) denoted mild, moderate, and severe modifications, respectively.

### Measurement of malondialdehyde (MDA) concentration

Thiobarbituric acid (TBA) assay described by Buege and Aust[41] was employed to measure the concentration of malondialdehyde (MDA) in the liver tissue homogenates, where MDA reacts with TBA in acidic medium forming a pink colored adduct measured spectrophotometrically at 535 nm. The test was carried out in the following manner: First, prepare (TBA-TCA-HCl reagent (chromagen)) by dissolving 15 g of trichloroacetic acid TCA (15% final) and 375 mg of TBA (0.37% final) in 50 ml $H_2O$, followed by addition of 2.08 ml of concentrated HCl (0.25 N final). Then, the mixture was heated to 70 °C in a water bath (to help dissolution of TBA), then the volume completed to 100 ml with distilled $H_2O$, and covered during prepartion to prevent change in concentration. The reaction was created by mixing 0.5 mL of liver homogenate, 0.5 ml of distilled water and 2 ml of TBA/TCA /HCl reagent. The solution was subjected to thermal treatment in a water bath for 15 min. Following the chilling process, allow cooling and centrifugation at a speed of 5000 revolutions per minute for 10 min to isolate the colored supernatant layer. The pink product's absorbance was quantified at 535 using a UV-visible spectrophotometer, with a blank sample for comparison. The concentration of MDA in the liver tissue was quantified as nmol/mg protein. By employing this procedure, the concentration of MDA was assessed in the liver tissue homogenates, serving as an indicator of lipid peroxidation levels.

*Measurement of superoxide dismutase (SOD) activity*
The level of superoxide dismutase (SOD) activity in liver homogenate was determined using the method outlined by Nandi and Chatterjee[42]. This technique relies on the capacity of SOD to hinder the spontaneous oxidation of pyrogallol under alkaline conditions. Below is a concise overview of the process: 100 μL of the liver sample was added to 2 mL of a solution containing 20 mmol Tris-HCL buffer (containing 1 Mm EDTA at a pH of 8.2). The reaction was started by introducing 100 μL of a recently generated 15 mM pyrogallol solution. The absorbance at a wavelength of 420 nm was continually measured for a duration of 2 min, with measurements obtained during the time interval of 1 to 3 min. The results were quantified as tissue homogenate units per milligram of protein. A single unit of SOD activity is determined as the quantity of enzyme needed to reduce the auto-oxidation of pyrogallol by 50%. The results were expressed as tissue homogenate units per milligram of protein.

*Measurement of glutathione content and catalase activity*
The glutathione content (GSH) and catalase activity in the liver homogenate were measured using Bio diagnostic kits obtained from 29 Tahreer St., Dokki, Giza, Egypt. The kits utilized were Cat. No. GR 25 11 for glutathione (GSH) and Cat. No. CA 25 17 for catalase. The measurements were carried out according to the manufacturer's instructions.

Biuret reagent using Spetcrum-diagnostics kit obtained from Obour city industrial area, Cairo, Egypt, was employed to determine the total protein content of the liver tissues. The kit utilized was Cat. No. 310,001. Measurements were taken using a PerkinElmer Lambda 25 UV/VIS spectrophotometer and reported as absorbance readings.

*Western blot analysis*
The tissues were crushed into a uniform mixture using Tris lysis solution that consisted of 400 mM NaCl, 0.5% Triton X-100, and 50 mM Tris pH 7.4. Additionally, Protease Inhibitor Cocktail (Biospes, China) was included. The process of homogenization was conducted for 30 min at a temperature of 4 °C. The residual tissue was eliminated using centrifugation at a speed of 10,000 revolutions per minute for 10 min at a temperature of 4 °C. The protein concentration was subsequently measured using a BCA Protein Assay Kit (Thermo Fisher Scientific, USA) by the instructions provided by the manufacturer. Subsequently, equal quantities of protein (60 mg of total protein in each lane) that had undergone separation using 10% SDS-polyacrylamide gel electrophoresis were deposited onto a PVDF membrane (Millipore, Merk, USA)[43]. The membranes were obstructed with a solution containing 5% non-fat milk in TBST buffer for 1 h at ambient temperature. Subsequently, the membranes underwent a washing process and were then subjected to overnight incubation at a temperature of 4 °C with the primary antibodies: anti-Nrf2 (Biospes, China; dilution 1:200; CAT# YPA1865), anti-NF-B p65 (Cell Signaling Technologies; dilution 1:1000, CAT# 8242), or anti-actin (Cell Signaling Technologies; dilution 1:1000, CAT# 7074). After undergoing another round of washing, the membranes were then exposed to the suitable alkaline phosphatase-conjugated secondary antibody (1:5000, Novus Biologicals, LLC, Littleton, CO, USA) for 1 h. The bands were observed using the BCIP/NBT substrate detection Kit from Genemed Biotechnologies, Inc., located in California, USA. Actin served as an internal reference for protein loading, and the resulting bands were compared to actin using Fiji ImageJ (2.16.0) software, http://imagej.net/software/fiji/ (NIH, USA).

*Quantification of Proinflammatory cytokine, TNF-α*
The levels of TNF-α in the liver were quantified using ELISA kits obtained from Elabscience® (CAT# E-EL-R0019, 14780 Memorial Drive, Suite 108, Houston, Texas, 77079, USA), according to the manufacturer's instructions.

## Statistical analysis
The statistical study was conducted using IBM's SPSS software, (version 25.0, Chicago, IL, USA). The graphs were made using GraphPad Prism 9 software (San Diego, CA, USA). The mean ± standard error means (SEM) were employed to represent the data. The data's normal distribution was evaluated using the Shapiro-Wilk test. A one-way analysis of variance (ANOVA) was performed, followed by Tukey's post-hoc analysis. P value $< 0.05$ is considered a significant difference.

## Results
### GA, GLA, and their combination improved body weight gain and liver weight in AZM-treated rats
Figure 1 shows the experimental groups' body weight gain, liver weight, and liver index values. Administration of AZM to rats significantly reduced body weight gain and liver weight ($P < 0.05$), but no changes was detected in the liver index. However, administering AZM concurrently with GA, GLA, and their combination significantly increased the rats' indices, indicating a very efficient intensification of these indicators.

### GA, GLA, and their combination attenuated liver injury in AZM-treated rats
After receiving AZM, the rats' blood serum levels of ALT, AST, and ALP significantly increased. Specifically, there was an approximately 131.86% increase in ALT, a 75.20% increase in AST, and a 153.64% increase in ALP when compared to the control group of rats. Serum albumin levels decreased significantly by 55.19% compared to the control group ($p < 0.05$) (Fig. 2). The AZM + GA group demonstrated a significant decrease in serum ALT, AST, and ALP activity compared to the ASM group, by 43.83%, 30.13%, and 50.73%, respectively. In comparison to the AZM group, the AZM + GLA group exhibited significantly lower serum levels of ALT, AST, and ALP (43.47%, 26.54%, and 53.79%, respectively). Furthermore, we observed a significant reduction in serum ALT, AST, and ALP values in the AZM + GA + GLA group. When compared to the AZM group, the levels of ALT, AST, and ALP dropped by 56.64%, 31.16%, and 58.64%, respectively. Serum albumin levels in the AZM + GA,
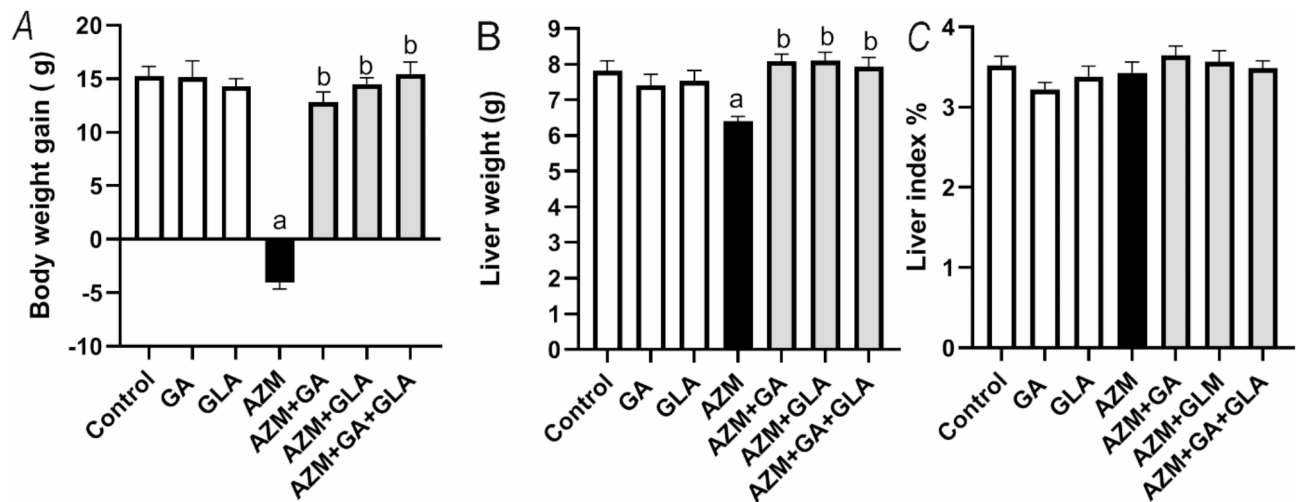
**Fig. 1.** Effect of GA, GLA, and their combination on (**A**) body weight gain, (**B**) liver weight, and (**C**) liver index in AZM-treated rats. The results are presented as the mean ± SEM ($n = 6$). A one-way ANOVA was utilized, followed by Tukey's post-hoc analysis with a significant threshold of $P < 0.05$. [a]$P < 0.05$; significantly different from the control group; [b]$P < 0.05$; significantly different from the AZM group. Where GA, GLA, and AZM denotes gallic acid, glycerihetenic acid, as well as azithromycin respectively.

AZM + GLA, and AZM + GA + GLA groups were considerably higher than in the AZM group (115.9%, 108.26%, and 128.44%, respectively) (Fig. 2D). This data demonstrates that the AZM + GA + GLA group is the most protected against AZM-induced liver damage.

### GA, GLA, and their combination alleviated the histological changes in the livers of AZM-treated rats

The histopathological study of liver tissues confirmed the biochemical assay results. The control, GA, and GLA groups all had typical hepatic structures, as shown in Fig. 3A&B for the control group, and in Fig. 3C&D for the GA and GLA groups. The hepatic structure included classic hepatic cords, centrally positioned veins (CV), and a portal region (PA) with intact blood sinusoids. The livers of rats given AZM showed severe necrosis and fatty degeneration. Both the portal (Fig. 3E, F, and G) and central areas (H) displayed vacuolated cytoplasm and necrosis. The AZM sections showed proliferating bile ducts, inflammatory cell infiltration, and significant portal vein congestion. Figure 3I&J shows mild necrosis and vacuolization in the portal area following GA and AZM treatment. Rat liver sections treated with AZM and GLA showed focal cellular necrosis, mild inflammation, and vacuolated cytoplasm in the portal region (Fig. 3K & L). The hepatic cells in the portal and central venous areas of rat liver slices treated with AZM and GA with GLA retained their structural integrity. However, a few hepatocytes contained vacuoles and minor foci of necrosis, as well as mildly proliferating bile ducts (Fig. 3M, N, and O). Figure 4 shows that AZM treatment significantly increased the liver histopathology score compared to the normal group ($P < 0.05$). However, in the AZM + GA, AZM + GLA, and AZM + GA + GLA groups, the liver histopathology score was significantly lower than in the AZM treatment.

### GA, GLA, and their combination attenuated oxidative stress in the livers of AZM-treated rats

In the AZM group, the amount of MDA in the liver rose by 97.7% ($p < 0.05$), but SOD and CAT activity dropped by 607.46% and 87.11%, respectively, compared to the control group (Fig. 5). Compared to the AZM group, the AZM + GA, AZM + GLA, and AZM + GA + GLA groups had significantly lower hepatic MDA contents ($P < 0.05$) of 93.54%, 88.07%, and 96.27%, respectively. However, compared to the AZM group, these groups had considerably higher hepatic SOD activity by 133.3%, 135.6%, and 144.4%, as well as higher CAT activity by 259.42%, 219.23%, and 264.01%, respectively (Fig. 5). On the other hand, the AZM group's liver GSH content decreased by 90.40% ($p < 0.05$) compared to the control group. The AZM + GA, AZM + GLA, and AZM + GA + GLA groups had considerably higher hepatic GSH levels than the AZM group (367.26, 322.46%, and 410.21%, respectively). This data demonstrates that the AZM + GA + GLA group is the most protected against AZM-induced liver damage.

### GA, GLA, and their combination reduced inflammation in the livers of AZM-treated rats

GA and GLA's anti-inflammatory effects in rats treated with AZM were evaluated by assessing inflammatory markers like TNF-α and NF-kB (Fig. 6). The treatment with AZM raised the levels of TNF-α and NF-kB proteins in the liver by 771% and 581%, respectively, compared to the control group (p-value < 0.05). On the other hand, hepatic TNF-α and NF-kB expression levels were significantly decreased after treatment of animals with GA, GLA, and GA + GLA by about 63% and 42%, 54% and 29%, and 81% and 66%, respectively, compared to the AZM at p-value < 0.05. This data demonstrates that the AZM + GA + GLA group is the most protected against AZM-induced hepatic inflammation.
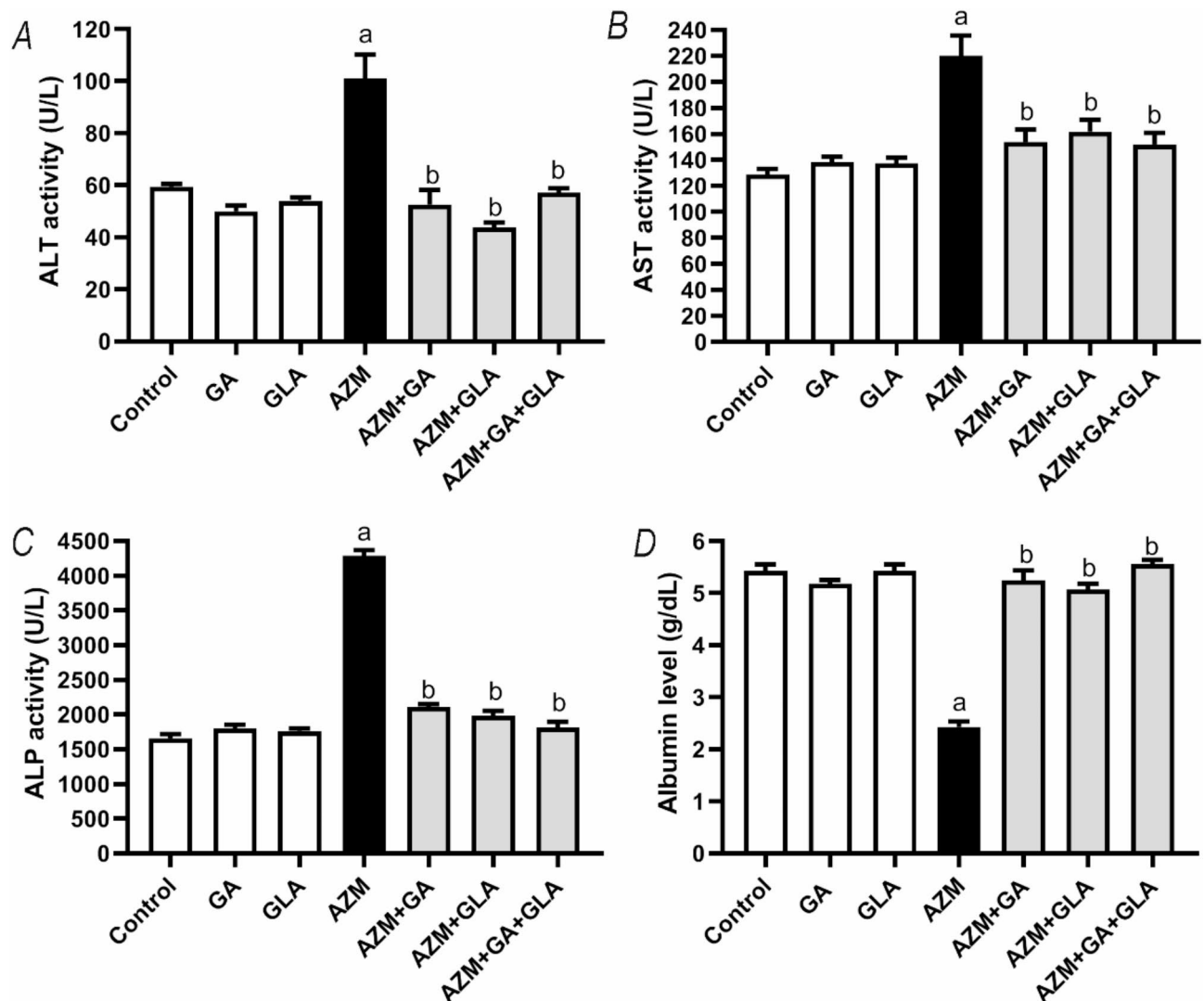
**Fig. 2**. Effect of GA, GLA, and their combination on AZM-induced liver toxicity in rats. The markers include (**A**) serum ALT activity, (**B**) serum AST activity, (**C**) serum ALP activity, and (**D**) serum albumin level. The data is displayed as the mean ± SEM ($n = 6$). We performed the ANOVA statistical analysis first, followed by Tukey's post-hoc analysis. A $P < 0.05$ indicates a significant difference from the control group, while b $P < 0.05$ indicates a significant difference from the AZM group.

### GA, GLA, and their combination attenuated the suppression of Nrf2 expression in the livers of AZM-treated rats

Western blot analysis revealed that the amount of Nrf2 protein in the livers of rats that were given AZM was 71% lower ($P < 0.05$) than in the control group (Fig. 7B). However, after pretreatment with GA, GLA, or GA + GLA, the Nrf2 expression levels in the liver of AZM-treated rats significantly increased by approximately 144%, 259.0%, and 297%, respectively, in comparison to the AZM group. (Figs. 7A and B).

### Discussion

Drug-induced acute liver injury is a major global health issue, often resulting in liver failure, the need for transplantation, and even death. To address this critical issue, the development and implementation of effective therapeutic interventions are urgently needed. Oxidative tissue injury and inflammation are key mechanisms driving the pathogenesis of acute liver injury[15]. Therefore, novel compounds with antioxidant and anti-inflammatory properties hold promise in protecting against liver dysfunction. In the present study, we investigated the potential health benefits of GA, GLA, and their combination in mitigating AZM-induced acute liver toxicity in rats. Our findings demonstrated that these compounds effectively alleviated oxidative stress, reduced inflammation, and prevented subsequent liver tissue damage.

Some drugs, particularly AZM, have a high risk of acute liver injury[10]. In our study, rats treated with AZM alone exhibited weight loss and reduced liver weight, indicative of systemic toxicity and metabolic disruption. In contrast, co-treatment with GA, GLA, or their combination led to increased body and liver weights, suggesting

that these compounds enhance liver metabolism and detoxification processes. Previous studies have reported that a routinely used antibiotic, like AZM often cause acute liver injury[13,14]. Animal studies have demonstrated that AZM-induced acute liver damage is associated with elevated circulating liver biomarkers, impaired liver function, and the development of histopathological alterations including hepatic degeneration, fatty changes, sinusoidal congestion, and inflammatory cell infiltration[9,37,44]. Similarly, we discovered that treating Wistar rats AZM at a dose of 30 mg/kg caused severe liver injury reflected in high levels of ALT, AST, and ALP. In our experimental model, elevated liver biomarkers were correlated with significant morphological abnormalities, including severe necrosis, fatty degeneration, proliferating bile ducts, and inflammatory cell infiltration. These observed changes in liver damage and structure align with findings from previous studies[9,37,44]. Hepatocyte necrosis and degeneration precede membrane disruption, resulting in the release of hepatic biomarkers into the bloodstream and their subsequent elevation in blood levels[45]. Thus, under hepatic stress conditions, elevated serum levels of hepatic enzyme markers serve as a sensitive indicator of increased hepatocyte membrane permeability and cellular damage[45]. In addition to hepatic damage, AZM-treated rats showed hepatic dysfunction, as evidenced by a reduced serum albumin levels. Our results demonstrate that GA, GLA, and their combinations confer protection against AZM-induced liver injury. Histological analysis confirmed these protective effects, as evidenced by the maintenance of normal liver enzyme levels (ALT, AST, and ALP) and albumin, alongside the preservation of liver tissue integrity. Different studies have revealed that GA provided hepatoprotective effects against damage induced by tert-butyl hydroperoxide[24], bisphenol[25], ethanol[26], and thioacetamide[27]. Similarly, GLA has been shown to protect liver cells from toxins such as carbon tetrachloride, 2-acetylaminofluorene, cyclophosphamide, methotrexate, and alpha-naphthyl isothiocyanate[31–33,35,46]. In this study, the AZM + GA + GLA group exhibits the highest level of protection against AZM-induced liver injury, as evidenced by the percentage of protection observed.

Oxidative stress and the antioxidant defense system play a critical role in drug-induced acute liver injury[16]. Under normal conditions, the antioxidant defense system - comprising SOD, CAT, and GSH - effectively neutralizes free radicals generated during the metabolism of toxic substances and medications[47,48]. Oxidative stress arises when there is an imbalance between free radicals and antioxidants are out of equilibrium[47]. Numerous investigations have demonstrated that AZM induces the production of ROS, leading to increased levels of lipid peroxidation products (MDA) and a reduction in antioxidant levels, including CAT, SOD, and GSH in the hearts and livers of treated animals[7,49]. Our findings revealed that AZM increased oxidative stress, as evidenced by markedly elevated MDA levels. Furthermore, we observed a consistent reduction in the activity of CAT and SOD, as well as decreased GSH concentrations, aligning with the results reported by Singh et al.[49]. The present study revealed that GA, GLA, and their combinations effectively increased antioxidant levels (GSH, CAT, and SOD) and reduced lipid peroxidation products (MDA) in liver tissue of rats treated with 30 mg/kg of AZM, highlighting their potentialantioxidant properties. For instance, GA has been shown to protect the liver against oxidative damage induced by chemicals like lead[23], thioacetamide[27], and carbon tetrachloride[38]. Similarly, GLA demonstrated the ability to scavenge ROS and mitigate oxidative stress in liver injury models involving valproic acid[50], cyclophosphamide[34], and methotrexate[35]. The percentage of protection further confirmed that the AZM group exhibited the highest protection against AZM-induced liver damage.

Analyzing the Nrf2-mediated pathway provides insights into the mechanisms underlying the antioxidant capabilities of GA and GLA. Both GA and GLA upregulate Nrf2, leading to enhanced expression and activity of antioxidant defense enzymes. This reduces the level of reactive oxidants and mitigate their associated cellular damage. Pretreatment of rats with GA, GLA, or their combination reversed the significant decline in Nrf2 protein expression in liver tissue induced by AZM. Consequently, upregulating Nrf2 enhances the production of antioxidant defense enzymes, thereby reducing reactive oxidants and minimizing cellular injury. Under oxidative stress, Nrf2 translocates to the nucleus and binds to the antioxidant response element (ARE), promoting the expression of enzymes involved in the synthesis of SOD, CAT, and glutathione[36]. Researchers have demonstrated that GA modulates the Nrf2 signaling pathway, offering protection against liver damage induced by tert-butyl hydroperoxide and ethanol[24,26]. Similarly, GLA's hepatoprotective effects against cyclophosphamide- and methotrexate-induced liver injury are mediated through the Nrf2-dependent antioxidant response[34,35]. Based on the percentage of protection, the AZM + GA + GLA group exhibited the highest level of protection against AZM-induced oxidative liver oxidative damage and the decline in Nrf2 protein expression.

Increased ROS generation play a major role in initiating pro-inflammatory signaling pathway. These pathways activate NF-kB, leading to the production of proinflammatory mediators and subsequent liver inflammation. Liu et al.[51] demonstrated that oxidative stress enhances NF-kB activity, resulting in the release of proinflammatory cytokines such as TNF-α. Studies have shown that substances like Valproic acid, 2-acetylaminofluorene, methotrexate, and thioacetamide increase NF-kB and proinflammatory cytokine levels, contributing to acute liver damage[33,35,50,52]. In our study, pre-treatment with GA and GLA in AZM-treated rats significantly reduced levels of NF-kB and TNF-α levels, confirming their protective effects against AZM-induced liver damage and highlighting their liver-specific anti-inflammatory properties. Previous studies have explored the anti-inflammatory effects of GA and GLA in various liver injury models. For instance, GLA treatment reduced TNF-α and NF-kB levels in rat model of cyclophosphamide- and methotrexate-induced acute hepatitis[34,35]. Similarly, Mohamed and Hafez[52] reported in 2023 that GA treatment reduced TNF-α, NF-kB, and other inflammatory mediators in thioacetamide-induced liver injury.

Furthermore, this study revealed a significant inverse relationship between Nrf2 and NF-kB in the livers of AZM-treated rats. The activation of Nrf2 was found to be crucial for the anti-inflammatory effects of GA and GLA. Nrf2 can directly inhibit NF-kB signaling and the production of pro-inflammatory cytokines, thereby exerting regulatory control over the inflammatory cascade. In vivo studies have highlighted the pivotal role of Nrf2 in managing inflammatory diseases across various systems[53]. The Nrf2 signaling pathway suppresses the activity of cytokines and other inflammatory mediators, influencing NF-kB expression and other networks
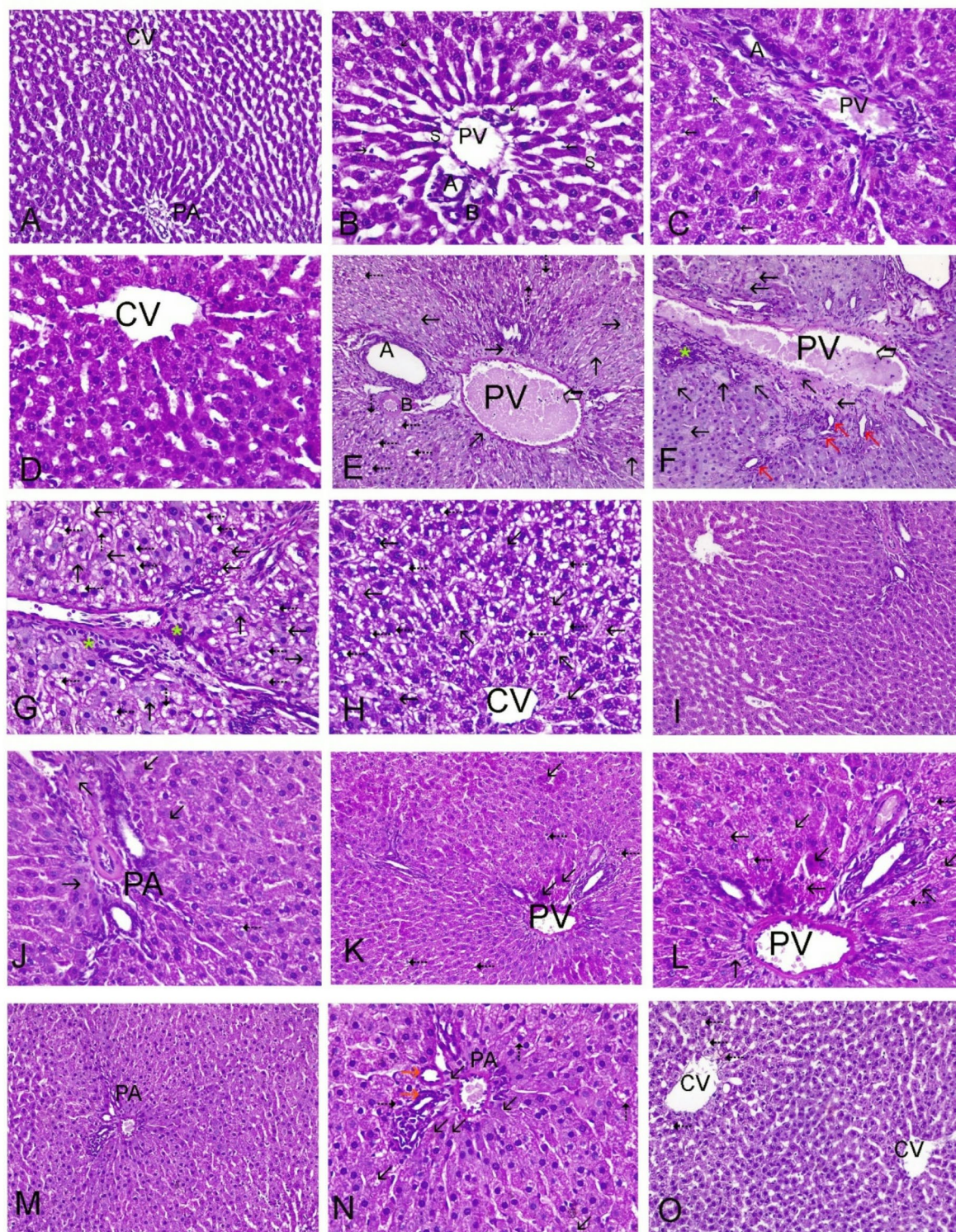
involved in inflammation regulations[53]. This concept is supported by several studies, including those by Jin et al.[50], Mahmoud et al.[35], Qi et al.[54], and Younis et al.[55], which demonstrate that certain phytochemicals with anti-inflammatory properties can effectively up-regulate Nrf2 and downregulate NF-kB. Collectively, GA and GLA and their combination may help mitigate AZM-induced liver damage by reducing the oxidative stress and inflammation through the upregulation of Nrf2 expression.

## Conclusions

In the present study, GA and GLA protected rats from AZM-induced liver damage. This hepatoprotection is closely associated with the upregulation of Nrf2, a transcription factor integral to cellular defence systems, which mitigates oxidative stress and inflammation caused by AZM. By reducing oxidative stress, GA and GLA prevent the accumulation of ROS that can damage liver cells. Additionally, their anti-inflammatory properties help

◀**Fig. 3**. Histopathological investigations of liver sections stained with H&E. Control groups (**A&B**), GA groups (**C**), and GLA groups (**D**) all had normal liver structures. (**A**) The liver's lobules have prominent interlobular septa with polygonal hepatocytes extending from the PA and CV (×200). (**B&C**) The portal region (PA) is comprised of the hepatic artery (**A**), the bile duct (**B**), and portal vein branches. Hepatocytes have eosinophilic cytoplasm and vesicular nuclei when they are visible. Flat endothelial cells and Kupffer cells (black arrows) line the sinusoidal spaces (S) between hepatocytes (×400). (**E**) The AZM group has a dilated portal vein (thick arrow), numerous necrotic areas (black arrows), hepatocyte vacuolization, and fatty degeneration (5). (**F**) The AZM group showed bile duct hyperplasia (red arrow), dilated portal vein (thick arrow), and necrosis with inflammatory cell infiltrations (*) (×400). (**G&H**) The AZM group (×400) exhibits severe necrosis (black arrows), hepatocyte vacuolization, fatty degenerations (5), and inflammatory cell infiltrations (*). (**I&J**) The histological structure of the AZM + GA group indicates a recovery to normal liver architecture along with some vacuolization, fatty degenerations (5) of the liver cells (×200, ×400), and minimal necrosis (black arrows). (**K&L**), The AZM + GLA group's histological structure shows necrotic patches in the portal areas (black arrows) (×200, ×400). The histological structure of the AZM + GA + GLA group is normal, with rare foci of necrosis (black arrows) and vacuolization (5) in the portal areas (M & N, ×200, ×400) and central vein area (O, ×200), as well as bile duct hyperplasia (red arrow).

counteract the inflammatory response triggered by AZM. However, the precise mechanisms though which GA and GLA modulate Nrf2 expression and exert their hepatoprotective effects require further investigation (Fig. 8).

Additional investigations are necessary to evaluate their efficacy and safety in clinical situations.
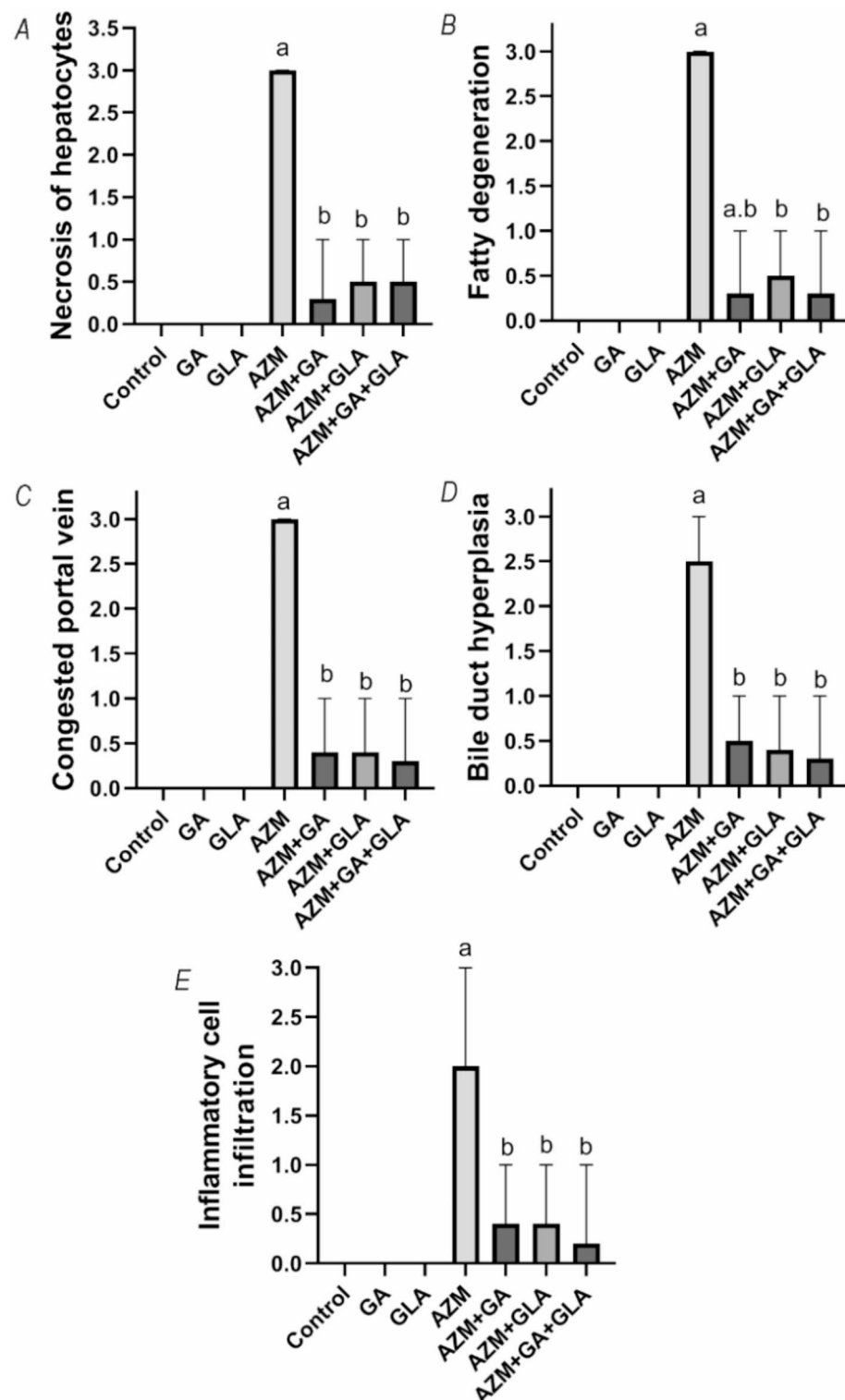
**Fig. 4**. Histopathological scores for (**A**) necrosis of hepatocytes, (**B**) fatty degeneration, (**C**) congested portal vein, (**D**) bile duct hyperplasia, and (**E**) inflammatory cell infiltrations, Values expressed as median ± 95% confidence interval for five animals in each group. Significance was determined by the non-parametric Kruskal-Wallis H test flowed by pairwise comparison:. [a]$P<0.05$; significantly difference from the control group; [b]$P<0.05$; significantly difference from the AZM group.
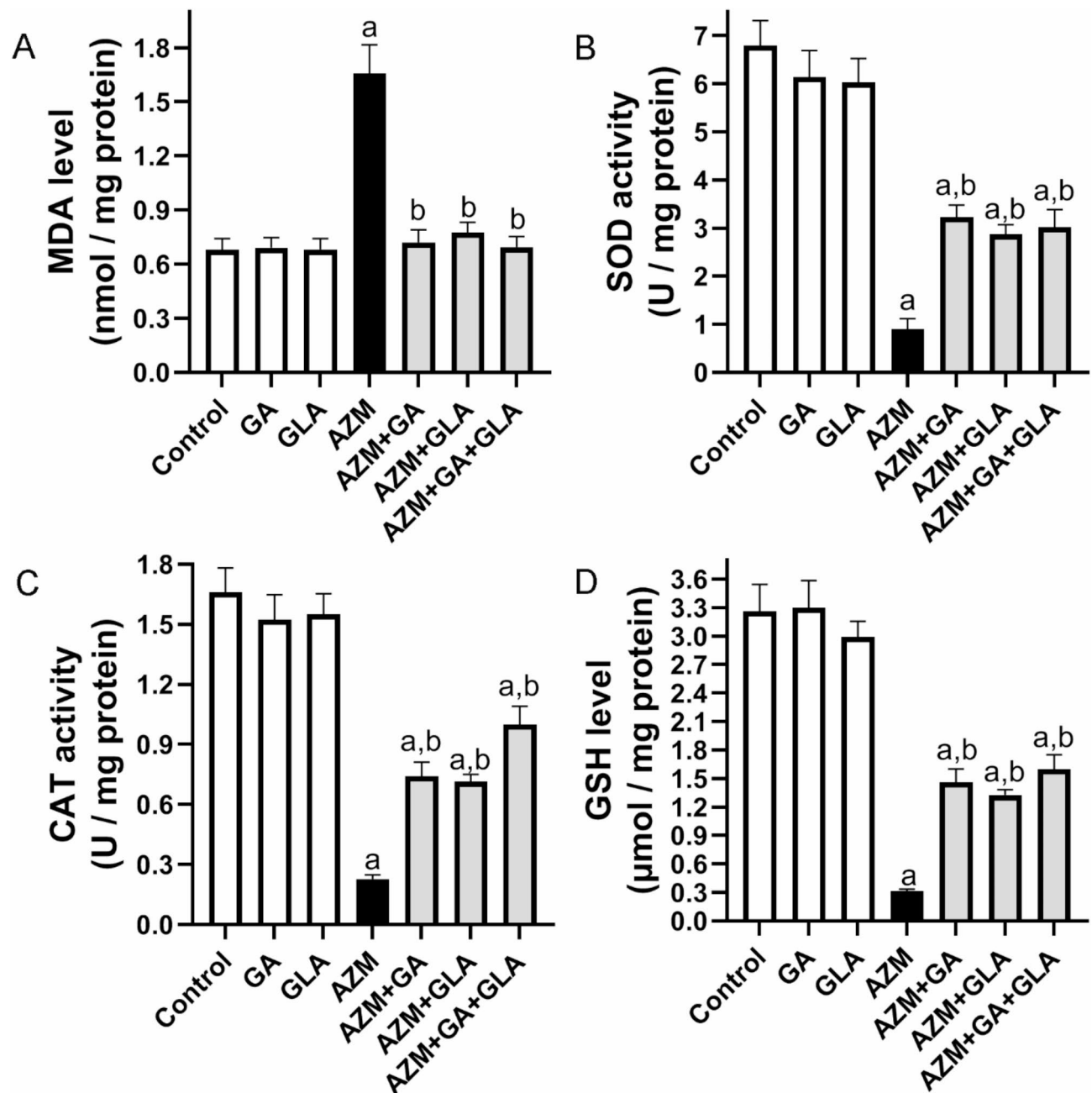
**Fig. 5**. Effect of GA, GLA, and their combination on the hepatic oxidative stress in AZM-treated rats. The oxidative markers include (**A**) MDA level, (**B**) SOD activity, (**C**) CAT activity, and (**D**) GSH level. The data is displayed as the mean ± SEM ($n = 6$). We performed the ANOVA statistical analysis first, followed by Tukey's post-hoc analysis. a P value < 0.05 indicates a significant difference from the control group, while b $P < 0.05$ indicates a significant difference from the AZM group.
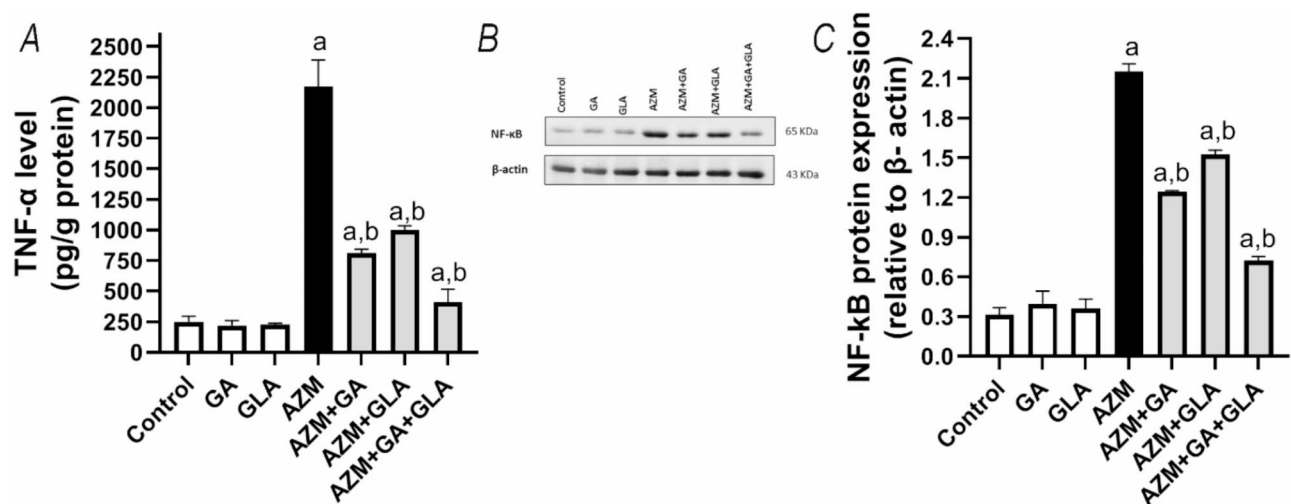
**Fig. 6**. Effect of GA, GLA and their combination on the hepatic inflammation in AZM-treated rats. (**A**) The expression level of TNF-α in the liver was determined by ELISA. (**B**) The expression level of NF-kB and B-actin in the liver was determined by western blotting. B-actin was used as an internal control. Original blots are presented in supplementary figure S1 and S2 (**C**) Quantitative analysis of the Nf-kB protein. Data are presented as the mean ± SEM of three independent experiments, performed in triplicate. a Significantly different from the control at a p-value < 0.05; b Significantly different from AZM at a p-value < 0.05.
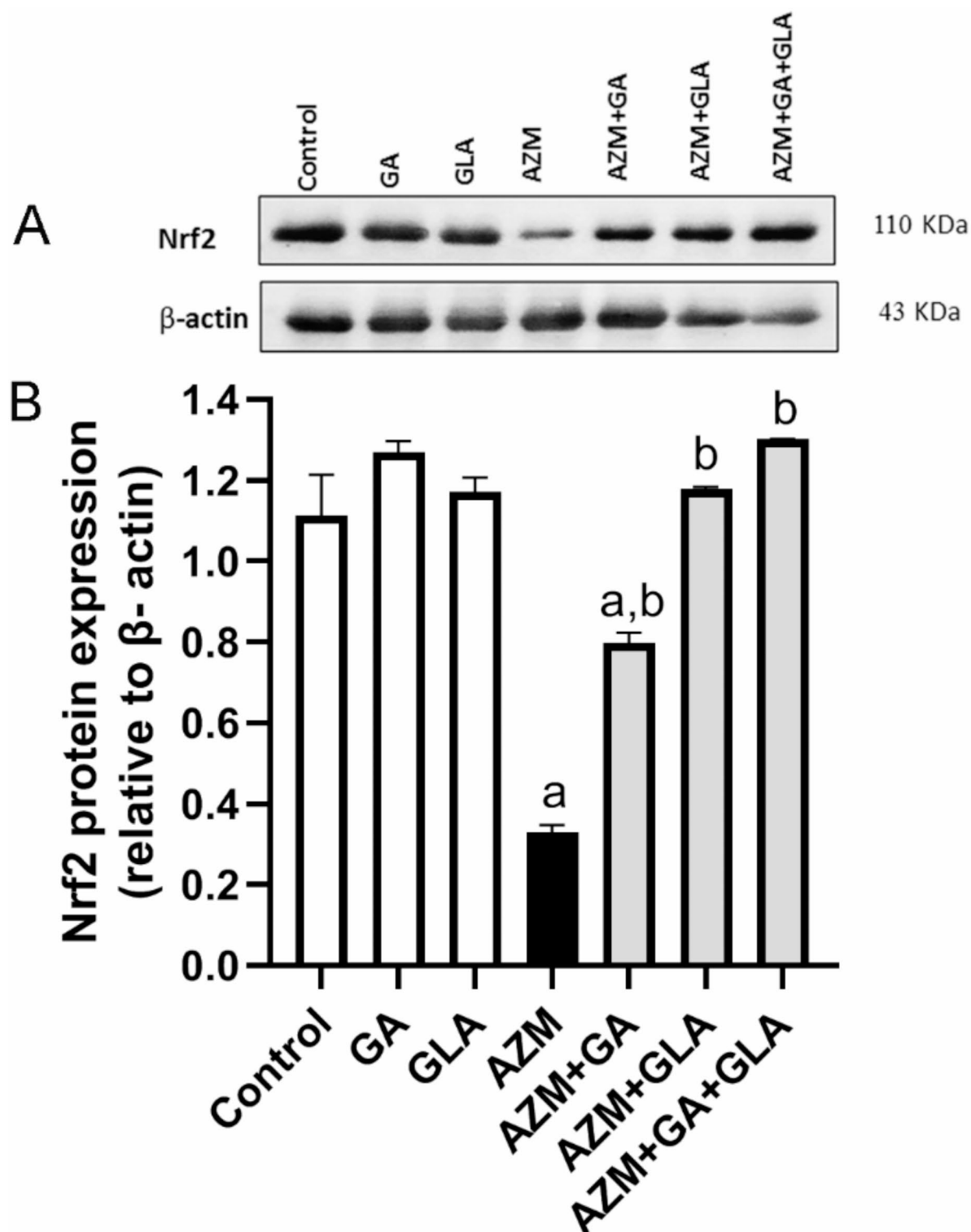
**Fig. 7**. (**A**) The expression level of Nrf2 and B-actin in the liver was determined by western blotting. B-actin was used as an internal control. Original blots are presented in supplementary figure S3 and S4 (**B**) Quantitative analysis of the Nrf2 proteins. Data are presented as the mean ± SEM of three independent experiments, performed in triplicate. a Significantly different from the control at a *p-value < 0.05;* b Significantly different from AZM at a *p-value < 0.05*.
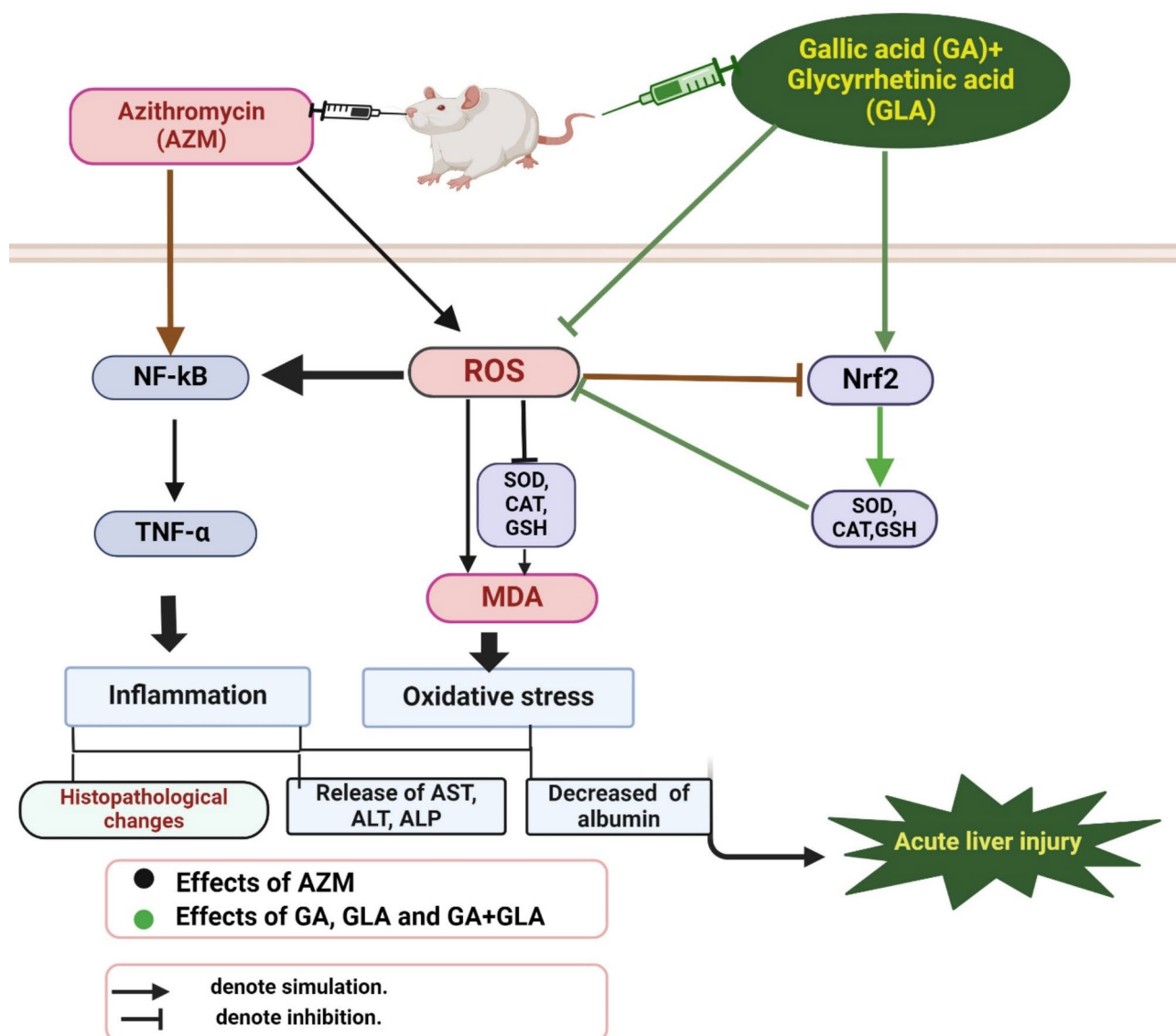
**Fig. 8.** The proposed mechanism of gallic acid and glycyrrhetinic acid action. Gallic acid and glycyrrhetinic acid protect rats from AZM-induced acute liver injury by modifying the Nrf2 and NF-kB signaling pathways. These modifying the Nrf2 and NF-kB signaling pathways reduce oxidative stress and inflammation caused by AZM. Created in BioRender, BioRender. https://BioRender.com/q89l287.

### Data availability

### References

1. Björnsson, H. K. & Björnsson, E. S. Drug-induced liver injury: Pathogenesis, epidemiology, clinical features, and practical management. *Eur. J. Intern. Med.* **97**, 26–31. https://doi.org/10.1016/j.ejim.2021.10.035 (2022).
2. Clinton, J. W. et al. Drug-Induced liver injury: Highlights and controversies in the recent literature. *Drug Saf.* **44**, 1125–1149. https://doi.org/10.1007/s40264-021-01109-4 (2021).
3. Jin, C. et al. Treatment responses to Azithromycin and Ciprofloxacin in uncomplicated Salmonella Typhi infection: A comparison of clinical and Microbiological data from a controlled human infection model. *PLoS Negl. Trop. Dis.* **13**, e0007955 (2019).
4. Bal, A. M. Macrolide antibiotics. (2022).
5. Zhai, G., Li, M., Wang, Y. & Wu, J. Drug-induced liver disturbance during the treatment of COVID-19. *Front. Pharmacol.* **12**, 719308 (2021).
6. Firth, A. & Prathapan, P. Azithromycin: The first broad-spectrum therapeutic. *Eur. J. Med. Chem.* **207**, 112739 (2020).

7. Atli, O., Ilgin, S., Altuntas, H. & Burukoglu, D. Evaluation of Azithromycin induced cardiotoxicity in rats. *Int. J. Clin. Exp. Med.* **8**, 3681 (2015).
8. Hamza, R. Z. et al. Ascorbic acid ameliorates cardiac and hepatic toxicity induced by azithromycin-etoricoxib drug interaction. *Curr. Issues Mol. Biol.* **44**, 2529–2541 (2022).
9. Li, S. et al. Establishment of a new animal model of azithromycin-induced liver injury and study the molecular pathological change during the process. *Hum. Exp. Toxicol.* **35**, 511–525 (2016).
10. Ellison, C. A. & Blackwell, S. B. Acute hepatocellular injury associated with Azithromycin. *J. Pharm. Pract.* **34**, 493–496 (2021).
11. Danica, J. et al. Vanishing bile duct syndrome associated with Azithromycin in a 62-year-old man. *Basic. Clin. Pharmacol. Toxicol.* **106**, 62–65 (2010).
12. Martinez, M. A. et al. Clinical and histologic features of azithromycin-induced liver injury. *Clin. Gastroenterol. Hepatol.* **13**, 369–376 (2015).
13. Park, H. J., Seo, K. I. & Choi, Y. I. Liver transplantation for azithromycin-induced severe liver injury. *Korean J. Transplantation* **34**, 279–285 (2020).
14. Choi, Y. I., Moon, H. H., Jo, J. H. & Shin, D. H. Liver transplantation for azithromycin-induced severe liver injury: A case report. *Korean J. Transplantation* **35**, 130 (2021).
15. Reyes-Gordillo, K., Shah, R. & Muriel, P. Oxidative stress and inflammation in hepatic diseases: Current and future therapy. *Oxid. Med. Cell. Longev.* **2017** (2017).
16. Villanueva-Paz, M. et al. Oxidative stress in drug-induced liver injury (DILI): From mechanisms to biomarkers for use in clinical practice. *Antioxidants* **10**, 390 (2021).
17. Zhang, M. M., Qiao, Y., Ang, E. L. & Zhao, H. Using natural products for drug discovery: The impact of the genomics era. *Expert Opin. Drug Discov.* **12**, 475–487 (2017).
18. Govea-Salas, M. et al. *In the Liver* 317–322 (Elsevier, 2018).
19. Aglan, H. A., Ahmed, H. H., El-Toumy, S. A. & Mahmoud, N. S. Gallic acid against hepatocellular carcinoma: An integrated scheme of the potential mechanisms of action from in vivo study. *Tumor Biol.* **39**, 1010428317699127 (2017).
20. Gao, J., Hu, J., Hu, D. & Yang, X. A role of Gallic acid in oxidative damage diseases: A comprehensive review. *Nat. Prod. Commun.* **14**, 1934578X19874174 (2019).
21. Jadon, A., Bhadauria, M. & Shukla, S. Protective effect of Terminalia Belerica Roxb. And Gallic acid against carbon tetrachloride induced damage in albino rats. *J. Ethnopharmacol.* **109**, 214–218 (2007).
22. Latief, U., Husain, H., Mukherjee, D. & Ahmad, R. Hepatoprotective efficacy of Gallic acid during Nitrosodiethylamine-induced liver inflammation in Wistar rats. *J. Basic. Appl. Zool.* **76**, 31–41 (2016).
23. Reckziegel, P. et al. Antioxidant protection of Gallic acid against toxicity induced by Pb in blood, liver and kidney of rats. *Toxicol. Rep.* **3**, 351–356 (2016).
24. Feng, R. B., Wang, Y., He, C., Yang, Y. & Wan, J. B. Gallic acid, a natural polyphenol, protects against tert-butyl hydroperoxide-induced hepatotoxicity by activating ERK-Nrf2-Keap1-mediated antioxidative response. *Food Chem. Toxicol.* **119**, 479–488 (2018).
25. Dutta, M. & Paul, G. Gallic acid protects rat liver mitochondria ex vivo from bisphenol A induced oxidative stress mediated damages. *Toxicol. Rep.* **6**, 578–589 (2019).
26. Zhou, Y. et al. Gallic acid protects against ethanol-induced hepatocyte necroptosis via an NRF2-dependent mechanism. *Toxicol. Vitro.* **57**, 226–232 (2019).
27. Hussein, R. M., Anwar, M. M., Farghaly, H. S. & Kandeil, M. A. Gallic acid and ferulic acid protect the liver from thioacetamide-induced fibrosis in rats via differential expression of miR-21, miR-30 and miR-200 and impact on TGF-β1/Smad3 signaling. *Chemico-Biol. Interact.* **324**, 109098 (2020).
28. Sundaresan, S. et al. Gallic acid attenuates cadmium mediated cardiac hypertrophic remodelling through upregulation of Nrf2 and PECAM-1signalling in rats. *Environ. Toxicol. Pharmacol.* **87**, 103701 (2021).
29. Li, X., Sun, R. & Liu, R. Natural products in licorice for the therapy of liver diseases: Progress and future opportunities. *Pharmacol. Res.* **144**, 210–226 (2019).
30. Shinu, P. et al. Pharmacological features of 18β-glycyrrhetinic acid: A pentacyclic triterpenoid of therapeutic potential. *Plants* **12**, 1086 (2023).
31. Chen, S., Zou, L., Li, L. & Wu, T. The protective effect of glycyrrhetinic acid on carbon tetrachloride-induced chronic liver fibrosis in mice via upregulation of Nrf2. *PLoS One* **8**, e53662 (2013).
32. Yang, Y. et al. Protective effects of hepatocyte-specific glycyrrhetic derivatives against carbon tetrachloride-induced liver damage in mice. *Bioorg. Chem.* **72**, 42–50. https://doi.org/10.1016/j.bioorg.2017.03.009 (2017).
33. Hasan, S. et al. 18-β glycyrrhetinic acid alleviates 2-acetylaminofluorene-induced hepatotoxicity in Wistar rats: Role in hyperproliferation, inflammation and oxidative stress. *Hum. Exp. Toxicol.* **34**, 628–641 (2015).
34. Mahmoud, A. M. & Al Dera, H. S. 18β-Glycyrrhetinic acid exerts protective effects against cyclophosphamide-induced hepatotoxicity: Potential role of PPARγ and Nrf2 upregulation. *Genes Nutr.* **10**, 41. https://doi.org/10.1007/s12263-015-0491-1 (2015).
35. Mahmoud, A. M., Hussein, O. E., Hozayen, W. G. & Abd El-Twab, S. M. Methotrexate hepatotoxicity is associated with oxidative stress, and down-regulation of PPARγ and Nrf2: Protective effect of 18β-Glycyrrhetinic acid. *Chem. Biol. Interact.* **270**, 59–72. https://doi.org/10.1016/j.cbi.2017.04.009 (2017).
36. Iranshahy, M., Iranshahi, M., Abtahi, S. R. & Karimi, G. The role of nuclear factor erythroid 2-related factor 2 in hepatoprotective activity of natural products: A review. *Food Chem. Toxicol.* **120**, 261–276. https://doi.org/10.1016/j.fct.2018.07.024 (2018).
37. Paulose, P. et al. Ameliorative effect of vitamin E on Azithromycin induced biochemical and histological changes in liver tissue of rats. *Adv. Anim. Vet. Sci.* **4**, 85–91 (2016).
38. Ojeaburu, S. & Oriakhi, K. Hepatoprotective, antioxidant and, anti-inflammatory potentials of Gallic acid in carbon tetrachloride-induced hepatic damage in Wistar rats. *Toxicol. Rep.* **8**, 177–185 (2021).
39. Bancroft, J. D. & Gamble, M. *Theory and Practice of Histological Techniques* (Elsevier health sciences, 2008).
40. Ibrahim Fouad, G. & Ahmed, K. A. Curcumin ameliorates doxorubicin-induced cardiotoxicity and hepatotoxicity via suppressing oxidative stress and modulating iNOS, NF-κB, and TNF-α in rats. *Cardiovasc. Toxicol.* **22**, 152–166 (2022).
41. Buege, J. A. & Aust, S. D. *In Methods in Enzymology* 52302–310 (Elsevier, 1978).
42. Nandi, A. & Chatterjee, I. Assay of superoxide dismutase activity in animal tissues. *J. Biosci.* **13**, 305–315 (1988).
43. Towbin, H., Staehelin, T. & Gordon, J. Electrophoretic transfer of proteins from polyacrylamide gels to nitrocellulose sheets: Procedure and some applications. *Proc. Natl. Acad. Sci.* **76**, 4350–4354 (1979).
44. Usadadia, S., Patel, J., Vihol, P. & Urkude, A. Protective effect of Quercetin on Azithromycin induced hepatotoxicity and nephrotoxicityin Wistar rats. *Int. J. Curr. Microbiol. Appl. Sci.* **9**, 2926–2934 (2020).
45. Plaa, G. & Zimmerson, H. Evaluation of hepatotoxicity: physiological and biochemical measures of hepatic function. *Compr. Toxicol.* **9**, 97–109 (1997).
46. Wang, H. et al. Glycyrrhizin and glycyrrhetinic acid inhibits alpha-naphthyl isothiocyanate-induced liver injury and bile acid cycle disruption. *Toxicology* **386**, 133–142 (2017).
47. Liguori, I. et al. Oxidative stress, aging, and diseases. *Clin. Interv Aging,* 757–772 (2018).
48. Jomova, K. et al. Reactive oxygen species, toxicity, oxidative stress, and antioxidants: Chronic diseases and aging. *Arch. Toxicol.* **97**, 2499–2574 (2023).

49. Singh, H., Prakash, A., Kalia, A. & Majeed, A. B. A. Synergistic hepatoprotective potential of ethanolic extract of Solanum xanthocarpum and Juniperus communis against Paracetamol and Azithromycin induced liver injury in rats. *J. Traditional Complement. Med.* **6**, 370–376 (2016).

50. Jin, J. et al. Role of Nrf2 activation and NF-κB Inhibition in valproic acid induced hepatotoxicity and in diammonium glycyrrhizinate induced protection in mice. *Food Chem. Toxicol.* **73**, 95–104 (2014).

51. Liu, T., Zhang, L., Joo, D. & Sun, S. C. NF-κB signaling in inflammation. *Signal. Transduct. Target. Therapy*. **2**, 1–9 (2017).

52. Mohamed, E. K. & Hafez, D. M. Gallic acid and Metformin co-administration reduce oxidative stress, apoptosis and inflammation via Fas/caspase-3 and NF-κB signaling pathways in thioacetamide-induced acute hepatic encephalopathy in rats. *BMC Complement. Med. Ther.* **23**, 265 (2023).

53. Ahmed, S. M. U., Luo, L., Namani, A., Wang, X. J. & Tang, X. Nrf2 signaling pathway: Pivotal roles in inflammation. *Biochim. Et Biophys. Acta (BBA)-Molecular Basis Disease* **1863**, 585–597 (2017).

54. Qi, W. et al. Cardamonin protects against doxorubicin-induced cardiotoxicity in mice by restraining oxidative stress and inflammation associated with Nrf2 signaling. *Biomed. Pharmacother* **122**, 109547 (2020).

55. Younis, N. S., Elsewedy, H. S., Shehata, T. M. & Mohamed, M. E. Geraniol averts methotrexate-induced acute kidney injury via keap1/Nrf2/HO-1 and MAPK/NF-κB pathways. *Curr. Issues Mol. Biol.* **43**, 1741–1755 (2021).

## Author contributions

## Funding

## Declarations

## Competing interests

The authors declare no competing interests.

## Additional information

**Supplementary Information** The online version contains supplementary material available at https://doi.org/10.1038/s41598-025-93120-3.

**Correspondence** and requests for materials should be addressed to A.A.H. or A.A.

**Reprints and permissions information** is available at www.nature.com/reprints.

**Publisher's note** Springer Nature remains neutral with regard to jurisdictional claims in published maps and institutional affiliations.